Control of binocular gaze in a high-precision manual task

CrossMark

Matteo Valsecchi *, Karl R. Gegenfurtner

Justus-Liebig Universität Giessen, Abteilung Allgemeine Psychologie, Otto-Behaghel-Strasse 10F, D-35394 Giessen, Germany

ARTICLE INFO

ABSTRACT

We investigated the precision of binocular gaze control while observers performed a high-precision manual movement, which involved hitting a target hole in a plate with a hand-held needle. Binocular eye movements and the 3D-position of the needle tip were tracked. In general the observers oriented their gaze to the target before they reached it with the needle. The amplitude of microsaccades scaled with the distance of the needle tip. We did not find evidence for the coordination of version and vergence during microsaccades which could be expected if those movements displaced gaze between the needle and the target hole. In a control experiment observers executed small saccades between marks on a slanted plane. Even when the observers executed saccades as small as the microsaccades in the needle experiment, we observed a coordinated displacement of the point of gaze on the horizontal and depth axis. Our results show that the characteristics of eye movements such as the frequency and amplitude of microsaccades are adapted online to the task demands. However, a coordinated control of version and vergence in small saccades is only observed if a movement of gaze on a slanted trajectory is explicitly instructed.

1. Introduction

Humans are often faced with tasks which require an online coordination of eye and hand movements, such as manipulating static objects or intercepting moving ones (e.g. Land, 2006, 2009). Most often in everyday tasks the eyes are directed to task-relevant locations before the hand, or the tool that extends it, reaches them. For instance, in the process of making a sandwich our eyes will fixate the area where the bread is about to be cut by the knife (Hayhoe et al., 2003). This is a general strategy which observers apply both in pointing tasks (Desmurget et al., 1998) and in more complex tasks, as soon as the observers learn how to perform them (Sailer, Flanagan, & Johansson, 2005).

Generally, the tasks we have to fulfill require us to move our hands or to use our hands to move objects over relative large distances. This implies that if we would keep our eyes on the initial position, the target position would be viewed peripherally. Peripheral vision is characterized by lower acuity (Wertheim, 1894), so it is convenient to perform at least one saccade and foveate the target position. Sometimes, however, we are confronted with tasks which require us to produce extremely small but precise movements of our hands or fingers, typical examples being threading a needle, assembling a clock, removing a splinter or aiming a rifle. Under those conditions most of the relevant objects or object parts would

be viewed foveally, and the question arises as to whether a precise control of gaze position is still required. One class of eye movements which potentially could contribute to orient gaze over small distances is microsaccades. In particular, it has long been debated whether in such tasks microsaccades take the role that saccades have when we visually explore our environment, i.e. orienting gaze towards relevant locations. The first suggestion in this sense came from Steinman et al. (1973) and the first study to address this question was conducted by Winterson and Collewijn (1976). They found that microsaccade frequency was reduced while observers tried to thread a needle or aim a rifle and concluded that microsaccades were not likely of any use in such high-acuity tasks. This conclusion was supported by the results of a subsequent study where observers performed a high-acuity task which did not require any motor response (Bridgeman & Palca, 1980). Furthermore, Kowler and Steinman (1977, 1979) failed to show any improvement in the performance of observers trying to count the elements within a 30 arcmin uniform array when microsaccades were allowed. At this point the general view was that microsaccades were a somewhat puzzling aspect of oculomotor behavior. On the other side, evidence suggesting that microsaccades and saccades might have quite a lot in common was available very early and has been accumulating over the years (for a recent review see Martinez-Conde, Otero-Millan, & Macknik, 2013). Notice however that it has been questioned whether this applies to the extremely small microsaccades (under 10–13 min of arc) that were typically observed in the

early studies where optical lever devices were used as opposed to the now more common video-based, scleral coil or dual Purkinje eye trackers (Collewijn & Kowler, 2008). The first evidence connecting microsaccades and large-scale saccades emerged as Zuber, Stark, and Cook (1965) showed that microsaccades and saccades have similar kinematic profiles, suggesting a common origin within the oculomotor system. Moreover, Timberlake et al. (1972) showed that small saccades can occur in response to displacements of the fixation point as small as 10 min of arc, and Haddad and Steinman (1973) found that observers were able to voluntarily produce saccades as small as the microsaccades they observed during fixation. More recently, neurophysiological studies connected the execution of microsaccades to the activity of cells in the rostral pole of the superior colliculus (e.g. Hafed, Goffart, & Krauzlis, 2009; Munoz & Wurtz, 1993). It has also been shown that the inactivation of the rostral Superior Colliculus induces a reduction in the frequency of saccades and microsaccades during fixation (Goffart, Hafed, & Krauzlis, 2012). The general picture is that oculomotor space is represented in a continuous retinotopic map in the SC, from caudal neurons coding for large saccades to rostral neurons coding for small saccades (Hafed, 2011). Crucially, a few behavioral studies again suggested that microsaccades might be functionally equivalent to saccades. Microsaccades can occur for instance while observers scan natural images (Mergenthaler & Engbert, 2010; Otero-Milian et al., 2008) and their kinetic properties are not qualitatively different from the ones of microsaccades executed during fixation or large explorative saccades (Otero-Milian et al., 2008). Furthermore, if the size of the images is decreased, so do the amplitude and peak velocity of saccades, smoothly approaching the parameters of fixational microsaccades (Otero-Millan et al., 2013). Most importantly for the purpose of the current study, new evidence has emerged detailing the role of microsaccades in high-acuity visual tasks. Ko, Poletti, and Rucci (2010) measured eye movements while observers performed a needle-threading task in a simulated environment. Although they replicated the finding by Winterson and Collewijn (1976) and Bridgeman and Palca (1980) that the rate of microsaccades decreases towards the end of a trial, they were able to show that in such a task microsaccades contribute to displacing the line of gaze between relevant locations (i.e. the thread and the needle). Towards the end of the trial microsaccades became smaller in size and fewer in number because the two objects were substantially overlapping. This result is perfectly justified if one considers that visual acuity is not homogeneous even within the foveola and drops already 10 arcmin away from the preferred retinal locus of fixation (Poletti, Listorti, & Rucci, 2013).

Most of the studies that have been used in the past to investigate eye movements in high-precision tasks involved either stimuli presented on a screen (Ko, Poletti, & Rucci, 2010; Kowler & Steinman, 1977, 1979; Poletti, Listorti, & Rucci, 2013) or objects which were aligned on the frontoparallel plane (Bridgeman & Palca, 1980) and recording was normally monocular. Nonetheless everyday tasks can require looking at different depth levels and, at least when large saccades have to be performed, there is clear evidence that eye movements can be coordinated binocularly (e.g. Malinov et al., 2000). Binocular oculomotor coordination is potentially important in tasks where the precise position of objects in space has to be estimated from binocular disparity, indeed Ukwade, Bedell, and Harwerth (2003a, 2003b) showed that stereopsis is degraded as soon as vergence error produces a pedestal disparity of around 1.5′. It has long been known that fixational microsaccades are binocular (e.g. Ditchburn, 1955; Møller et al., 2002; Otero-Millan, Macknik, & Martinez-Conde, 2014; Schulz, 1984; St.Cyr & Fender, 1969), but it is not clear whether microsaccades contribute to reduce vergence error during fixation (e.g. Engbert & Kliegl, 2004) or whether vergence errors are corrected

mostly through slow control (e.g. Møller, Laursen, & Sjolie, 2006). Recent evidence supports the idea that fixational saccades can reduce the amount of vergence error induced by pictorial cues to depth (Pérez Zapata, Aznar-Casanova, & Supèr, 2013). Finally, Van Horn and Cullen (2012) demonstrated that at least at the level of the brainstem, premotor neurons code integrated commands for version and vergence during microsaccades, similarly to what has been observed in the case of large-scale saccades.

In summary, there is a consistent body of evidence supporting the idea that oculomotor control in high-precision tasks and in exploration tasks does not differ qualitatively and that in such tasks microsaccades might have a function similar to the one of saccades in exploration tasks. It is not yet known, however, whether this picture extends to binocular control of gaze in an everyday situation where the relevant objects in the workspace are on different depth planes. In the present study we measured binocular eye movements and the position of a needle which the observers tried to insert in a small hole in a plate by executing a precise movement on a slanted trajectory. As a comparison, we also studied the binocular control of eye movements as observers executed small saccades along a slanted plane.

2. Methods

2.1. Observers

Six students from the Justus-Liebig University of Giessen volunteered for the main experiment (all female, mean age 24.2 years). Five of the observers were available to take part in the instructed saccade experiment. All observers were right-handed and reported having normal visual acuity and binocular vision. Participants in the study provided written informed consent in agreement with the Declaration of Helsinki. Methods and procedures were approved by the local ethics committee LEK FB06 at Giessen University (proposal number 2009-0008).

2.2. Eye movements measurement and calibration

Eye movements were recorded binocularly at 500 Hz using an Eyelink II head-mounted infrared video-based system (SR Research, Missisauga, Canada). Head movements were limited, though not excluded by the use of a chin rest. The calibration procedure started with a standard 9-point calibration on a 23-in. Cathode Ray Tube monitor at 46 cm viewing distance. Subsequently, a custom 3D calibration procedure was performed. For the 3D calibration, observers were asked to look sequentially at a series of nine marks located on a mobile metal plate. The procedure was repeated three times with the plate positioned at three depth levels (see Fig. 1a). The distance between two adjacent points and between the depth levels was 30 mm so that the position of binocular gaze was acquired on a $3 \times 3 \times 3$ cubic grid with 60 mm side. The center of the cubic grid was approximately at 20 cm viewing distance.

The calibration procedure was followed by a validation procedure. To this purpose the plate was rotated 45° first clockwise and then counterclockwise. The observer looked in sequence at the three points at mid-height in each orientation (see Fig. 1b).

Both for the calibration and the validation procedures the experimented paced the acquisition by pressing a key when the observer looked at the instructed point. A specific point could be re-acquired if the observer had blinked or eye position signal was lost. For each point eye position was averaged in a 21 sample time window centered on the experimenter's keypress.

The binocular eye movements traces were codified in terms of head-referenced angles using the EyeLink software and the appro-
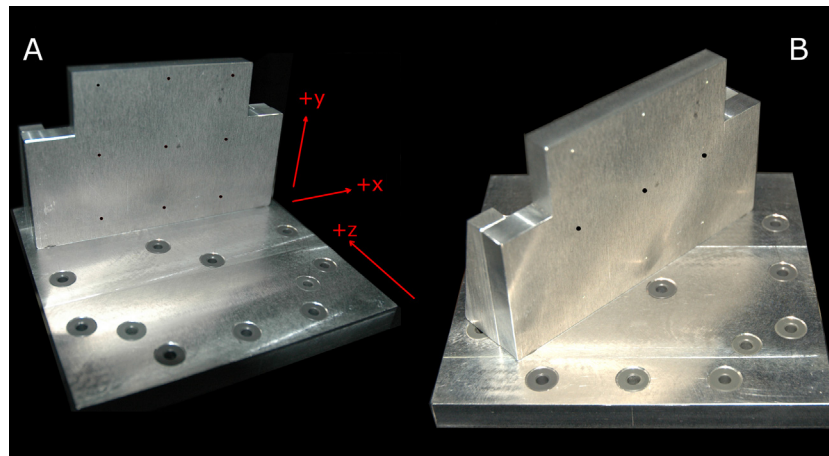
Fig. 1. Calibration (A) and validation (B) setup. For calibration observers were asked to look at the nine holes on the plate one after each other (marked with black circles in the image for display purposes), and the plate was located at three depth levels starting from the farthest. For the calibration of the Zebris system, the plate was rotated 90° counterclockwise and the tip of the needle was inserted in each hole so that the device holding the markers could pivot on the hole position. The procedure was again repeated three times positioning the plate left, center and right. For both calibrations the 27 measured points constituted a cubic grid (60 × 60 × 60 mm). The red arrows indicate the orientation of the calibration frame of reference. Notice that we codify larger depth from the observer's point of view as a larger z coordinate value. For the validation (B) the plate was rotated clockwise and counterclockwise (as in example) and the observers were asked to look at the three mid-height marks (here denoted by black circles) in sequence.

priate transformation, taking into account each observer's inter-pupil distance. A binocular point of gaze (POG) was defined as the midpoint of the shortest possible segment connecting the lines of gaze from the left and right eye (also see Pérez Zapata, Aznar-Casanova, & Supèr, 2013). The 27 POGs from the grid were aligned to a grid having the central point at the origin of the reference system and mapping right to the positive x axis, up to the positive y axis and depth to the positive z axis (left, up and depth as defined from the observers' point of view). The calibrated grid size was the same as the one of the physical grid (i.e. 60 mm side). The re-alignment of the eye position data was obtained using a 12 parameter model of the form:

$$y_j = w_{j1} + x_1 w_{j2} + x_2 w_{j3} + x_3 w_{j4} \tag{1}$$

where y is the calibrated position, x is the uncalibrated position, j is the space dimension (horizontal, vertical or depth) and w is the 12-element parameter array. A graphical description of the calibration transformation is depicted in Fig. 2.

For each observer and experiment we applied all of the calibration models to each validation dataset and chose the calibration model which produced the smallest RMS validation error.

The calibration/validation procedure was repeated every 10 trials in the main experiment and every 4 trials in the instructed saccade experiment. The best calibration for each validation dataset was applied to the binocular recordings from the corresponding set of data. In each trial we furthermore re-aligned the recordings of both the POG and the needle tip position by subtracting the position at the frame in which the needle contacted the plate. For each calibration which was used during the experiment we calculated the average RMS error of the calibrated points with respect to the physical position of the grid points (the error is represented by the red lines in Fig. 2B and C). The average calibration RMS error was 4.073 mm, whereas the standard deviation across calibrations was 0.75 mm. For comparison, in the viewing conditions of our setup, a purely horizontal POG displacement of 1 mm from the origin of the reference frame corresponds to an eye rotation of approximately .28°, meaning that if considered on the frontoparallel plane the average calibration error typically exceeded 1°. This value is about twice the error expected from the Eyelink II system (nominally <.5°), although a direct comparison is not viable since the POG computation takes vergence into account. Notice that
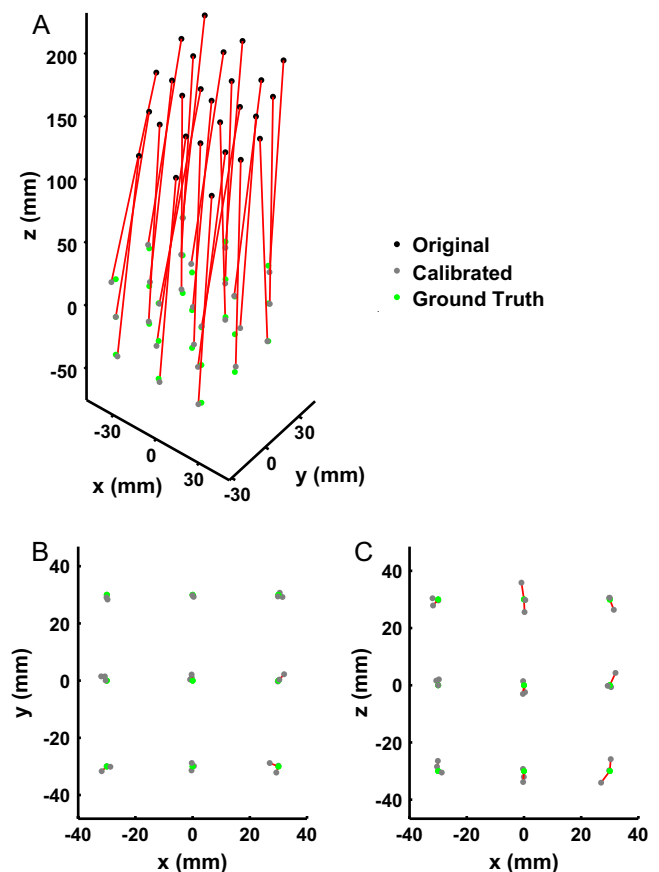

Fig. 2. Calibration transformation. (A) Example of a transformation actuated on eye movement dataset. (B) and (C) Calibration accuracy. The red segments represent the calibration residual error in x and y. The same calibration transformation was applied to the motion tracking data so as to align both eye and needle measurements in a common reference frame.

while the 4 mm error over a 60 mm grid ensures that we are able to measure the rough orientation of gaze shifts in 3D space, we cannot measure precisely the absolute position of gaze during a

trial down to the 1 mm scale. Throughout the data analysis we thus avoid drawing conclusions based on the absolute position of gaze at a given point, and rather concentrate on the change in gaze position associated with microsaccades.

Microsaccades were detected using a modified version of the algorithm introduced by Engbert and Kliegl (2003). The algorithm was applied requiring a minimum duration of 6 samples and a velocity threshold equal to 6 times the standard deviation of the velocity in a given epoch. This velocity threshold was found by Engbert and Mergenthaler (2006) to be optimal in the sense of detecting the largest number of non spurious events. Their finding was confirmed in our data (see Fig. 3A and C). The time intervals in which a blink was detected, extended to the preceding and following 50 ms, were excluded from the analysis. Rather than to the POG track, the algorithm was applied to the raw eye movement track of each eye. While microsaccades are generally considered conjugate eye movements (Engbert & Kliegl, 2004; Møller et al., 2002; Otero-Millan, Macknik, & Martinez-Conde, 2014) and the detection algorithm introduced by Engbert and Kliegl (2003) originally required the rejection of monocular microsaccades, we decided to keep monocular microsaccades in our sample. By definition, a relatively large vergence change during a microsaccade can only take place if eye velocity is smaller in one eye. By discarding monocular microsaccades we would have artificially reduced the amount of vergence change associated with microsaccades. We thus pooled together both monocular and binocular microsaccades (counting binocular microsaccades as a single event). We excluded from

the analysis of microsaccades the events whose amplitude exceeded 1.5°.

In order to ensure that our measurement system was sensitive enough to detect microsaccades of all sizes, we performed a surrogate data analysis similar to the one introduced by Engbert and Mergenthaler (2006). The surrogate data are produced by constrained random shuffling of the velocity traces, which aims at preserving the pattern of correlation of the original trace (Theiler et al., 1992). As a first step, we replicated the results of Engbert and Mergenthaler (2006) showing that, at least with data obtained with an Eyelink II system, the largest difference in the number of detected microsaccades between the original and surrogate data is obtained using a velocity threshold of around 5–7 standard deviations (Fig. 3A and C). We extended the analysis by computing the amplitude of the microsaccades detected in the original and surrogate data (for this purpose the position track was reconstructed by integrating the velocity traces). More microsaccades were detected in the original data as compared to surrogate data independently of amplitude, confirming that even the smallest saccades detected by our algorithm are not simply the result of noise. In particular, microsaccades with amplitude below 5′ are virtually absent from the surrogate data, whereas they appear, albeit in limited number, in the original data. Such small microsaccades correspond to movements with a markedly curved trajectory or to microsaccades which are markedly dysconjugate and are associated with displacements of the POG in depth, rather than on the frontoparallel plane. Notice that this result is in accordance with the fact that
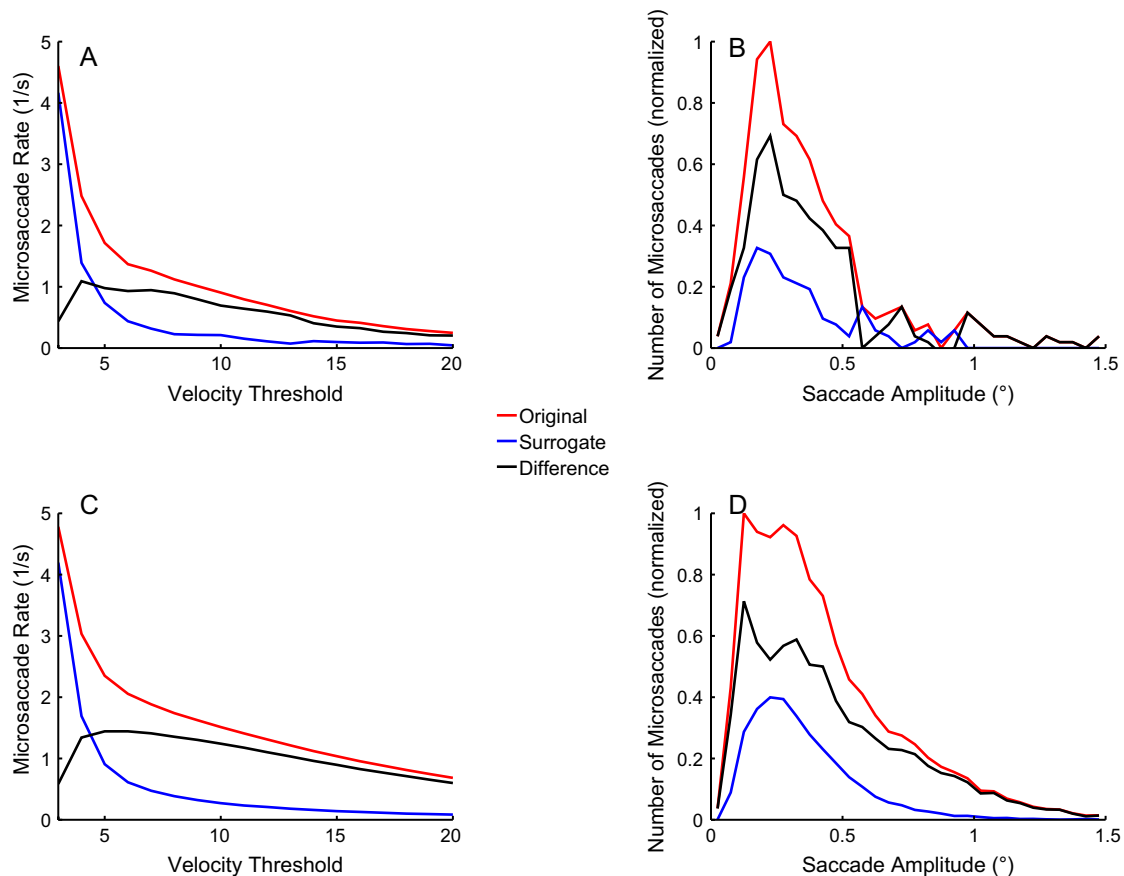

Fig. 3. Detection of microsaccades in surrogate data. (A) and (C) Detection rate as a function of the velocity threshold in the needle and control experiment, respectively. More microsaccades are detected in the original data at all velocity thresholds. The largest difference is obtained with threshold values between 4 and 7. (B) and (D) Number of microsaccades detected as a function of amplitude in the needle and control experiment, respectively (velocity threshold is set at 6). More microsaccades are detected in the original data in all amplitude bins. Notice that the results from the control experiment are more stable both because more data were collected in terms of recording time and because the observers produced more saccades according to the task.
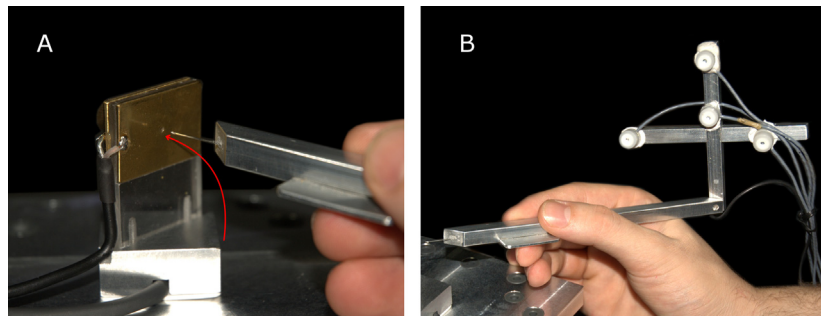
Fig. 4. Task setup. (A) Target device. Observers tried to hit the hole in the metal plate with the needle. If they succeeded a green light was illuminated inside the plate, if instead they hit the plate a red light was illuminated. The arrow describes the instructed movement from the corner of the target device to the target hole. (B) Needle holding device. Observers held the device in their right hand. Four ultrasound-emitting markers were fixed to the device enabling the tracking of the needle tip position.

the nominal resolution of the eye-tracker in the dark-pupil recording mode, which was used in the present study, is .01°, smaller than the overall length of most microsaccades.

2.3. Motion capture and calibration

The position of the needle point was tracked at 20 Hz by means of a Zebris ultrasound system (Zebris Medical GmbH, Isny i. Allgäu, Germany). Four markers were fixed to the needle holder which was held by the observer in the right hand (Fig. 4). The nominal resolution of the system is under .1 mm and the nominal accuracy, at the measurement distance used in the setup (around 1 m), is under 1 mm.

In order to calibrate the motion capture system we recorded the position of the markers fixed to the needle holder while the needle tip pivoted in each of the 27 possible calibration point positions (the plate was rotated 90% compared to the position used for the eye calibration, see Fig. 1a). For each calibration point the position of the pivoting point was reconstructed iteratively as the point in space which minimized the variation of its distances to the four markers. For each point we thus obtained a representation of the position of the pivoting point in space and for each frame a representation of the structure of the device. The final estimate of the device structure was obtained by re-aligning all structures with a rigid-body transformation (Challis, 1995; Soderkvist & Wedin, 1993) and then averaging all the marker positions. Similarly to the case of the eye movements recording, the needle tip position recordings were re-aligned to a common frame of reference with a 12 parameter calibration transformation (Eq. (1), Fig. 2). The procedure was performed once before testing the first five observers and again before testing the sixth. In the first case the RMS calibration error was 0.862 mm, in the second case it was 0.915 mm. Those values would correspond to around .31° if the error was expressed in terms of POG displacement on the horizontal plane.

2.4. Procedure: needle task

At the beginning of each trial, the observers were asked to position the needle tip (0.5 mm diameter) on the corner of the target plate (Fig. 4a). As the experimenter started the acquisition they were required to try to hit the center of a hole (1 mm diameter) in the center of a metal plate. The movement involved a displacement of approximately 32 mm (leftward, upward and towards larger depth). Observers were asked to perform the movement as precisely as possible rather than fast. If the observer managed to hit the center of the hole without touching the plate, a green LED was illuminated inside the plate, if they hit the plate a red LED was illuminated. Signals corresponding to the contact with the plate and the hole were co-recorded with the eye tracks. The diffi-
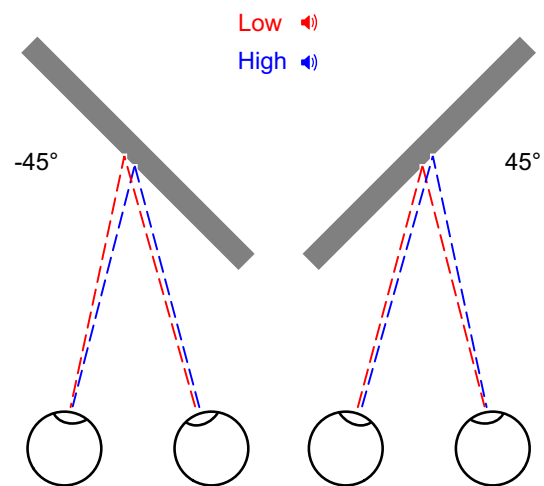

Fig. 5. Schematic task in the instructed saccade experiment. Observers rhythmically performed saccades between two marks on a surface rotated 45° either clockwise (left) or counterclockwise (right). The observers were required to fixate on the left mark when they heard the lower tone and on the right mark when they heard the higher tone.
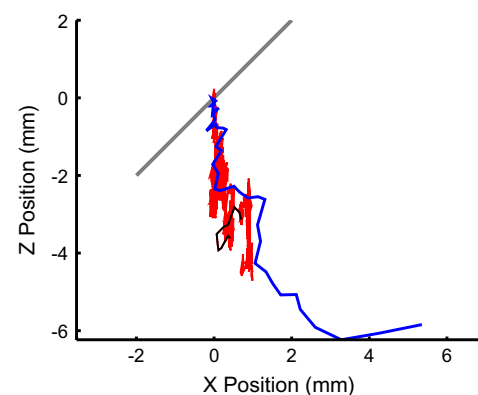

Fig. 6. Example of the displacement of gaze (red) and of the needle position (blue) on the horizontal plane during the last 2 s of one trial. The POG displacement during the microsaccade which was detected in the trial is marked in black. The gray bar denotes the orientation of the target plate. Both measures are re-aligned to the position at the time of contact. (For interpretation of the references to color in this figure legend, the reader is referred to the web version of this article.)

culty of the task could be adjusted by varying the depth of the target surface inside the plate hole. The experimenter increased the distance (thus imposing a more precise positioning of the needle)
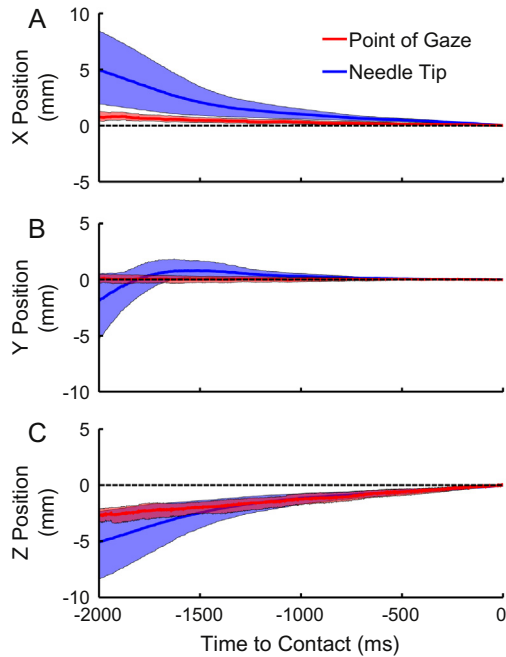
Fig. 7. Change in the position of the POG (red) and of the needle tip (blue) in the 2 s leading to the contact of the needle tip with the target along the X, Y and Z coordinates (panels A, B and C, respectively). Each track has been re-aligned to the position at the time of contact. It appears that the POG reached the final position earlier than the needle tip, especially on the vertical axis although a sizable adjustment of the vergence took place. Error bars are between-observer 95% confidence intervals. (For interpretation of the references to color in this figure legend, the reader is referred to the web version of this article.)

if the participant managed to perform the task correctly more than three times in a run of 10 trials and decreased it if less than three trials were successful. The experimenter could also flag the trial as incorrect if the observer failed to follow the instructions (e.g. the movement started before the instructed time). Testing lasted around 90 min including at least two breaks.

2.5. Procedure: instructed saccades

In the instructed saccade experiment the observers were required to perform saccades between vertical marks on a slanted surface (see Fig. 5). The surface was rotated 45° either clockwise or counterclockwise compared to the frontoparallel plane. On the plate were four pairs of marks spaced by 1, 2, 3 or 4 mm. The observer was told which marker pair to use before each trial. The pacing of the saccades was dictated by alternating tones of different pitch (440 or 523 Hz), with a tone-onset interval of 1000 ms (tone duration was 122 ms). Observers fixated the left mark when they heard the lower-pitch tone and the right mark when they heard the higher-pitch tone. 15 tones were presented in each trial. Testing
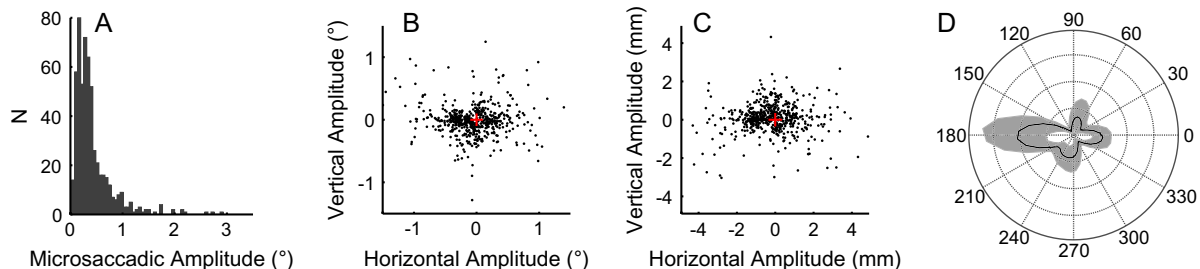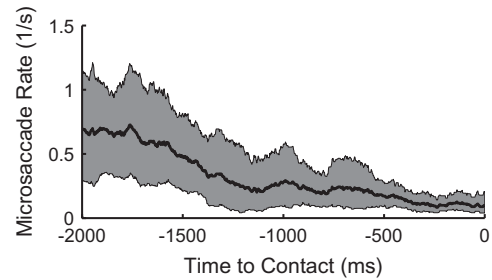

Fig. 9. Evolution of microsaccadic rate in the two final seconds of the trials. Microsaccade rate decreases as the needle approaches the final position. The shaded area represents the between-observer 95% confidence interval.

was conducted in two 60 min sessions on separate days, each one including at least one break.

3. Results

3.1. Needle task

As stated in Section 2, in each trial we asked our observers to move carefully the needle towards the hole in the plate. For each observer we collected on average 63.3 trials which were correctly calibrated and not flagged as erroneous. Furthermore, we rejected two trials (0.45%) in which the movement took less than 2 s. We did not instead examine the trials separately as a function of the task accuracy given that the task difficulty was such that the observers were incorrect most of the times. An example of the evolution of the position of the POG and needle tip in the last 2 s of a sample trial is represented in Fig. 6.

The average evolution of the position of the POG and of the tip of the needle in the 2 s leading to the contact between the needle tip and the target are depicted in Fig. 7. It appears that the POG approaches the final position earlier than the needle tip, for which a residual adjustment of the vertical position took place. The largest adjustment in POG took place in vergence (Fig. 7C), but the horizontal position (Fig. 7A) is also displaced towards positive values (i.e. to the right) which is the side from where the needle tip is approaching the target.

Most importantly, in a second step in the data analysis we investigated the role of miniature saccades. Overall we detected 547 microsaccades, each observer contributing between 25 and 192. Fig. 8A depicts the amplitude of microsaccades on the frontoparallel plane. The absolute amplitude of most microsaccades is below 1° and 97.3% of all microsaccades had amplitudes below the 1.5° threshold we set. As commonly observed the orientation of the movements is mostly horizontal (Fig. 8B and C). In particular in this case microsaccades towards the left tend to be overrepresented.

Fig. 8. Amplitude of all microsaccades on the frontoparallel plane. (A) Histogram of raw angular amplitude. (B) Raw angular displacement. (C) Calibrated POG displacement. (D) Polar histogram of directions (the shaded area represents the between-observer 95% confidence interval).
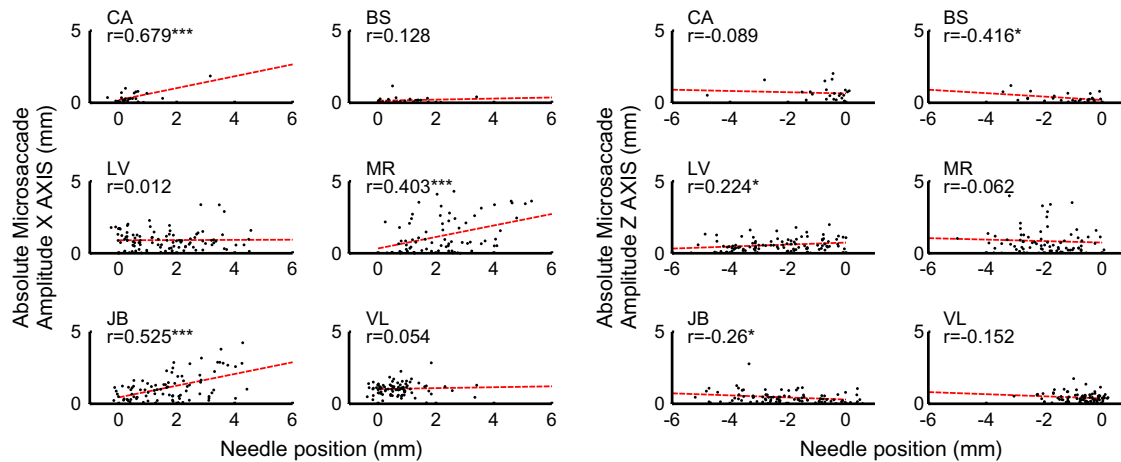
Fig. 10. Absolute amplitude of microsaccades for each observer as a function of the position of the needle tip at saccade onset relative to the position at the time of contact. Data for the *X* and *Z* axis are presented left and right, respectively. The regression line is depicted in red. Asterisks mark significant correlations (*$p < .05$, **$p < .01$, ***$p < .001$). Notice that although the relationship is not always significant in the individual data, in most of the cases (all but observer LV as far as the depth amplitude is concerned) the sign of the correlation is the expected one, i.e. microsaccade amplitude decreases as the needle approaches the target. (For interpretation of the references to color in this figure legend, the reader is referred to the web version of this article.)
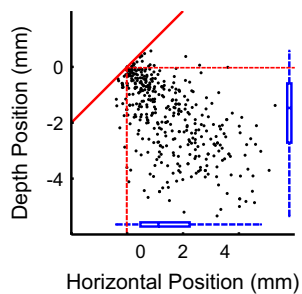

Fig. 11. Position of the needle tip relative to the contact position (the origin of the reference frame) when microsaccades were triggered. Each dot represents a microsaccade. Boxplots of the *X* and *Y* coordinates are depicted in blue. The red solid line indicates the predicted position of the plate. Notice that the needle tip was almost never located beyond the plate, suggesting that within this area of the workspace the localization was quite precise. The red dashed lines delimit the quadrant where the *X* and *Z* coordinates have opposite signs. (For interpretation of the references to color in this figure legend, the reader is referred to the web version of this article.)

Fig. 9 depicts the evolution of the rate of microsaccade occurrence. As expected based on previous findings from high-acuity visual tasks (Bridgeman & Palca, 1980; Ko, Poletti, & Rucci, 2010; Winterson & Collewijn, 1976) and coherent with the observation by Otero-Millan et al. (2013) that microsaccade rate is inversely related to the size of the actively explored area, the microsaccade rate decreases towards the end of the trial, i.e. when the distance between the needle tip and the target is minimal.

The fact that most microsaccades are horizontal, coupled with the notion that the needle approaches the target from a horizontal direction is suggestive of the fact that microsaccades might contribute to displace gaze between those two task-relevant dimensions. In order to have a more direct representation of the relationship between the occurrence of microsaccades and the ongoing needle manipulation, in Fig. 10 we plot the amplitude of microsaccades on the horizontal and depth axis as a function of the distance between needle and target. A relationship seems to be evident for most observers, consistent with the notion that the amplitude of microsaccades decreases as needle and target approach. Notice that for this and the following analysis we exclude the microsaccades observed when the needle distance to

the target is above 5.36 mm, which in our experimental setup would correspond to the POG displacement associated with a microsaccade of the maximum allowed amplitude of 1.5°.

The results we showed so far, indicating that the amplitude of microsaccades and their rate scale with the task requirements, and particularly with the distance between the task-relevant objects, are compatible with the results by Ko, Poletti, and Rucci (2010) who showed that microsaccades are used to explore the workspace during a high-acuity task. In the following we look for evidence of binocular control of microsaccades by examining the coordination of vergence and version during microsaccades.

As a first step we establish the geometry of the workspace at the time of microsaccades. Fig. 11 represent the position of the needle tip relative to the contact point on the horizontal plane as each microsaccade was triggered. In the vast majority (89.4%) of the cases the needle was located in the 4th quadrant of the horizontal plane of our frame of reference, i.e. the needle was locate on the right and nearer to the observer compared to the contact point. Within this frame of reference, if microsaccades would displace binocular gaze horizontally and in depth between the two task-relevant locations, we would expect to observe a negative correlation between the horizontal and depth displacement of the point of gaze during microsaccades.

The displacement of the POG on the horizontal plane associated with microsaccades is depicted in Fig. 12. The plot shows relatively large changes in vergence associated with microsaccades, but no clear relationship between horizontal displacement and depth displacement. Four observers show a negative correlation but two show the opposite pattern.[1] In principle, given that the needle tip is approaching from a position in front and to the right of the target hole (see Fig. 4A) and that the vast majority of microsaccades were triggered when the needle was in this zone (see Fig. 10), one would expect a negative relationship if both the change in vergence and version would be goal-directed and coordinated. The absence of a negative relationship between vergence and version during micro-

---

[1] The absence of an overall relationship between the two variables was confirmed by a Linear Mixed Model analysis (R package lme4) which we performed using the depth amplitude as a dependent variable, horizontal amplitude as a predictor and observer as a random factor. A chi square analysis showed no improvement in the model fit as the fixed effect of horizontal amplitude was added to a model containing a random intercept and a random effect of horizontal amplitude ($p = 0.472$) and when the fixed effect was added to a minimal model with only the random factor ($p = .4$). Adding the random effect of horizontal amplitude produced instead an improvement of the fit over the minimal model ($p < .001$).

saccades indicates that in this task microsaccades do not contribute to binocular coordination. Before concluding that this is the case, we validated the sensitivity of our measurement technique having observers execute small saccades along a plane slanted in depth.

3.2. Instructed saccade task

We approach the analysis of the instructed saccade task results in two different ways. First we identified and studied the small saccades which were executed accordingly to the task, so as to verify that observers were able to perform it. Subsequently, we pooled all the small saccades that were executed independently of the direction instructed by the task, which is a fairer comparison to the needle experiment where no specific instructions for eye movements were given.

The selection of the instructed saccades was based on their onset time relative to the sound, on their direction and on their amplitude. In particular, for each sound after the first in a trial we selected the saccade with the largest amplitude among those in the instructed direction taking place between 1 s before the sound onset and 1 s after the sound onset. On average 318.8 sound epochs were analyzed for each participant. We were able to associate a valid saccade to 41% of all epochs. Two examples of POG displacement on the horizontal plane associated with instructed saccades are depicted in Fig. 13.

The average change in POG associated with the saccades executed as a function of the instructed amplitude is depicted in Fig. 14. The movements appear to have approximately the correct amplitude on the horizontal axis, which is not surprising given that the movements were selected on the basis of this parameter. However, there is an evident modulation in the depth of the POG. The overall change in POG depth is slightly hypometric, particularly for the shortest movements (see Table 1) where the gain can be as low as 63% compared to the instructed amplitude of the movement. The most striking aspect of the plot in Fig. 14C is however that on top of the sudden change in vergence associated with the execution of the saccade, there is a slower evolution of fixation depth taking place even before the triggering of the saccade and well after the saccade ended, especially for the largest saccades.

The overall relationship between the POG displacement in depth and on the horizontal axis associated with saccades is depicted in Fig. 15. As stated in Section 2, the testing was conducted both with the plate oriented −45° and at 45° (see Fig. 5). In this case a movement with a perfect coordination of version and vergence would have produced a displacement with equal amplitude on both axes. Although the displacement on the horizontal axis is generally larger than on the depth axis, a significant linear relationship is observed also for the smallest movements, except for the movements which were executed when the distance between the marks was 1 mm and the plate was oriented at 45° (Fig. 15D).

As we anticipated, the small saccades we identified based on the current task instructions constitute a very selected subsample and might not be a fair comparison to the microsaccades executed in the absence of any specific task requirement in the needle experiment. We thus decided to avoid selecting the saccades based on their direction. Instead, for each observer we selected the smallest movements so as to obtain a subsample of saccades whose average horizontal amplitude was comparable to the one of the microsaccades we observed in the needle experiment. This was done by sorting the movements from the smallest to the largest based on the horizontal amplitude and adding them sequentially to the sub-sample until the sub-sample mean amplitude reached the value of 0.97 mm, i.e. the mean amplitude of microsaccades in the needle experiment. The relationship between horizontal and depth displacements for such movements is reported in Fig. 16. It is evident that an overall trend for a coordination of ver-
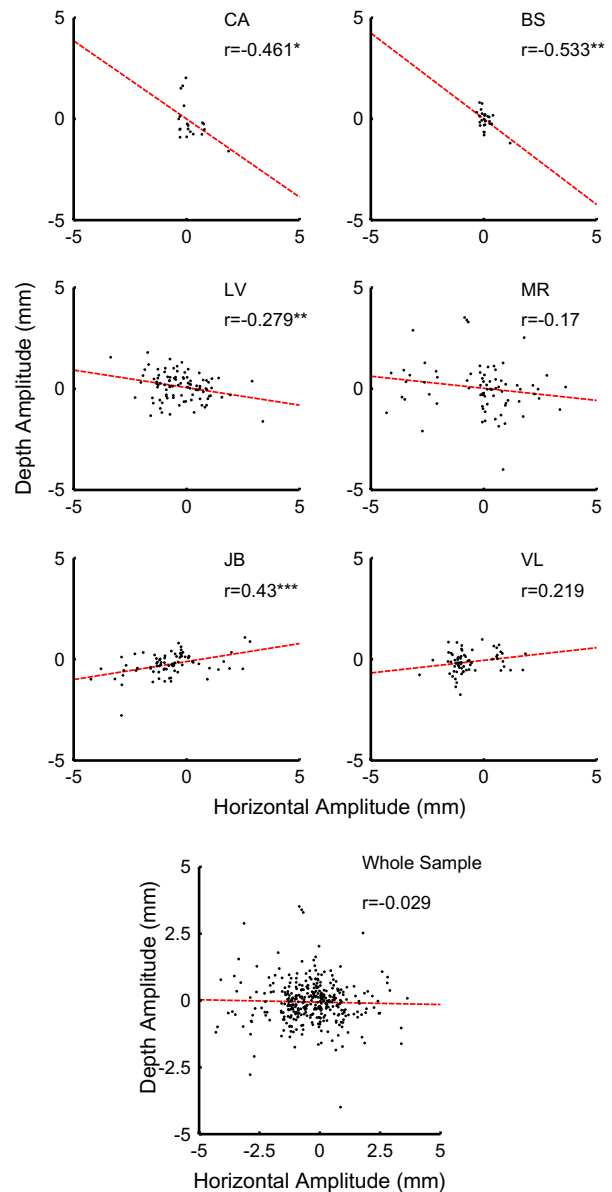

Fig. 12. Displacement of the POG on the horizontal plane associated with microsaccades. The regression line is depicted in red. Asterisks mark significant correlations (*p < .05, **p < .01, ***p < .001). A task-related coordination of version and vergence would produce a negative slope as the needle was approaching from the bottom-right quadrant of the horizontal plane (near-right from the observer's point of view). No clear pattern is evident overall, as two observers showed the opposite (in one case significant) trend. (For interpretation of the references to color in this figure legend, the reader is referred to the web version of this article.)

sion and vergence is present in the data. Only one in five observers did not show a significant correlation in the expected direction and the relationship was evident in the aggregate data[2], contrary to what was observed in the needle experiment (see Fig. 12).

---

[2] The presence of an overall relationship between the two variables was confirmed by a Linear Mixed Model analysis (R package lme4) which we performed using the depth amplitude as a dependent variable, horizontal amplitude as a predictor and observer as a random factor. A chi square analysis showed an improvement in the model fit as the fixed effect of horizontal amplitude was added to a model containing a random intercept and a random effect of horizontal amplitude (Orientation 1: p < .03; Orientation 2: p < .016) and when it was added to the minimal model with only the random intercept (Orientation 1: p < .001; Orientation 2: p < .001). Adding the random effect of horizontal amplitude also produced an improvement of the fit over a model with only the random factor (Orientation 1: p < .001; Orientation 2: p < .001).
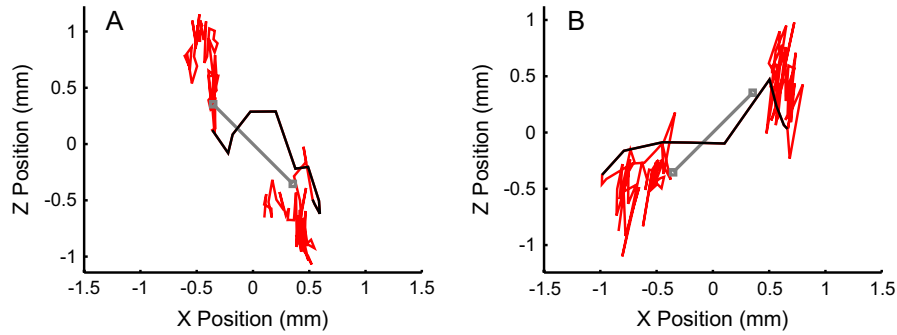
Fig. 13. Example of POG displacement during instructed saccades executed when the plate was oriented clockwise (A) and counterclockwise (B). The saccade trajectory is marked in black, the fixations preceding and following the saccades are marked in red. The average gaze position is set to 0 on both coordinates. For comparison, the gray bar represents the vector of the instructed movement, whose amplitude was 1 mm. (For interpretation of the references to color in this figure legend, the reader is referred to the web version of this article.)
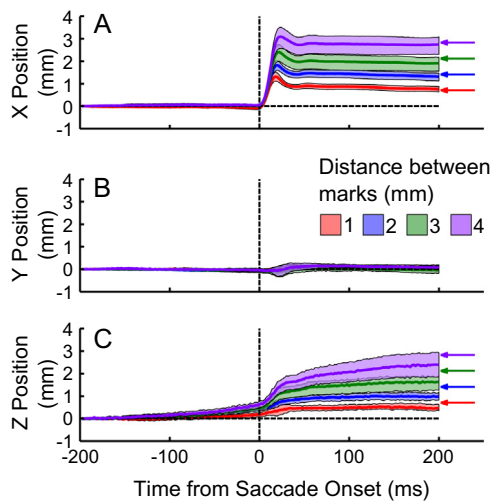

Fig. 14. POG displacement associated with saccades in the instructed saccade task, separately for the different distances between the marks. The arrows in A and C represent the size of the instructed POG displacement along the horizontal and vertical axes, respectively. No displacement in the vertical dimension was instructed (B). The tracks in A and C have been re-aligned before averaging so that positive values indicate a change in POG coherent with the instructed movement. Evidently the changes in vergence are hypometric, particularly for shorter movements, and the change has a rather slow dynamic both preceding and following the onset of the saccade. Error bars are between-observer 95% confidence intervals.

Evidently, the overall sample size is larger in the instructed saccade task (885 and 918 movements in the −45° and 45° orientations, respectively) as compared to the needle task (358 movements altogether), possibly due to the fact that observers were instructed to produce the small saccades. In order to have a fairer comparison between the two experiments, we re-conducted the analysis of the correlation in Fig. 16 on random subsamples of the data of different size (Fig. 17). Significant relationships with the expected slope sign were observed in most of the cases even with subsamples including as few as 200 movements, suggesting that the lack of a significant relationship in the needle experiment is not likely due to limited statistical power.

4. Discussion

The main aim of the present study was to investigate the binocular control of gaze during microsaccades as observers executed a precision hand movements involving displacement on all three spatial axes. Specifically, our observers repeatedly tried to insert the tip of a needle in a hole in a plate while we measured both binocular

Table 1
Gain of the saccadic amplitude on the horizontal and depth axes (average ± standard error of the mean) as a function of the distance between the marks. The gain was calculated based on the POG displacement across the 400 ms epoch centered on saccade onset.

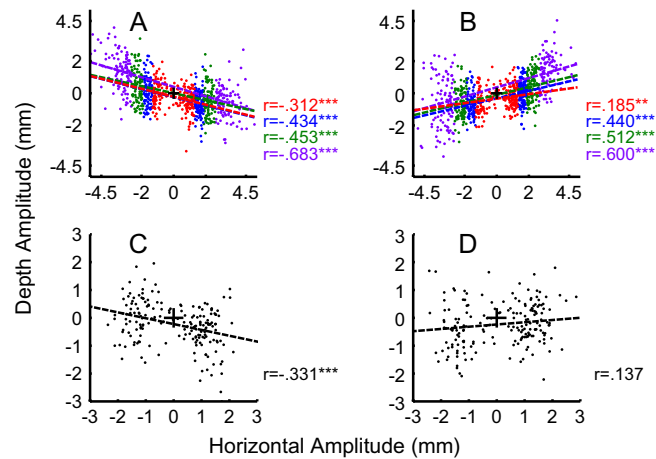|	Space axis	
	X	Z
Distance between marks		
1 mm	107.2 ± 9.6%	63.4 ± 12.2%
2 mm	93.1 ± 6.8%	70.9 ± 7.1%
3 mm	90 ± 8.4%	77.1 ± 9%
4 mm	97.2 ± 7.8%	84.6 ± 1.03%

Fig. 15. Amplitude of saccades on the horizontal plane. (A) and (B) Whole dataset. The color code denotes a quartile split of the movements based on their horizontal amplitude. (C) and (D) Saccades executed when the distance between the marks was 1 mm. (A) and (C) Movements executed with the plane oriented at −45°, (B) and (D) movements executed with the plane oriented at 45°. Dashed lines are linear fits. **p < .01, ***p < .001. (For interpretation of the references to color in this figure legend, the reader is referred to the web version of this article.)

ocular eye movements and the 3D position of the needle tip. In a control experiment we assessed binocular gaze coordination while observers executed small saccades along a slanted plane.

The main results of the study can be summarized as follows:

(1) The overall displacement of the point of gaze suggests a general strategy of oculomotor control which involves adjusting the vertical position first and subsequently the horizontal and depth position (similarly to what occurs for the needle tip).
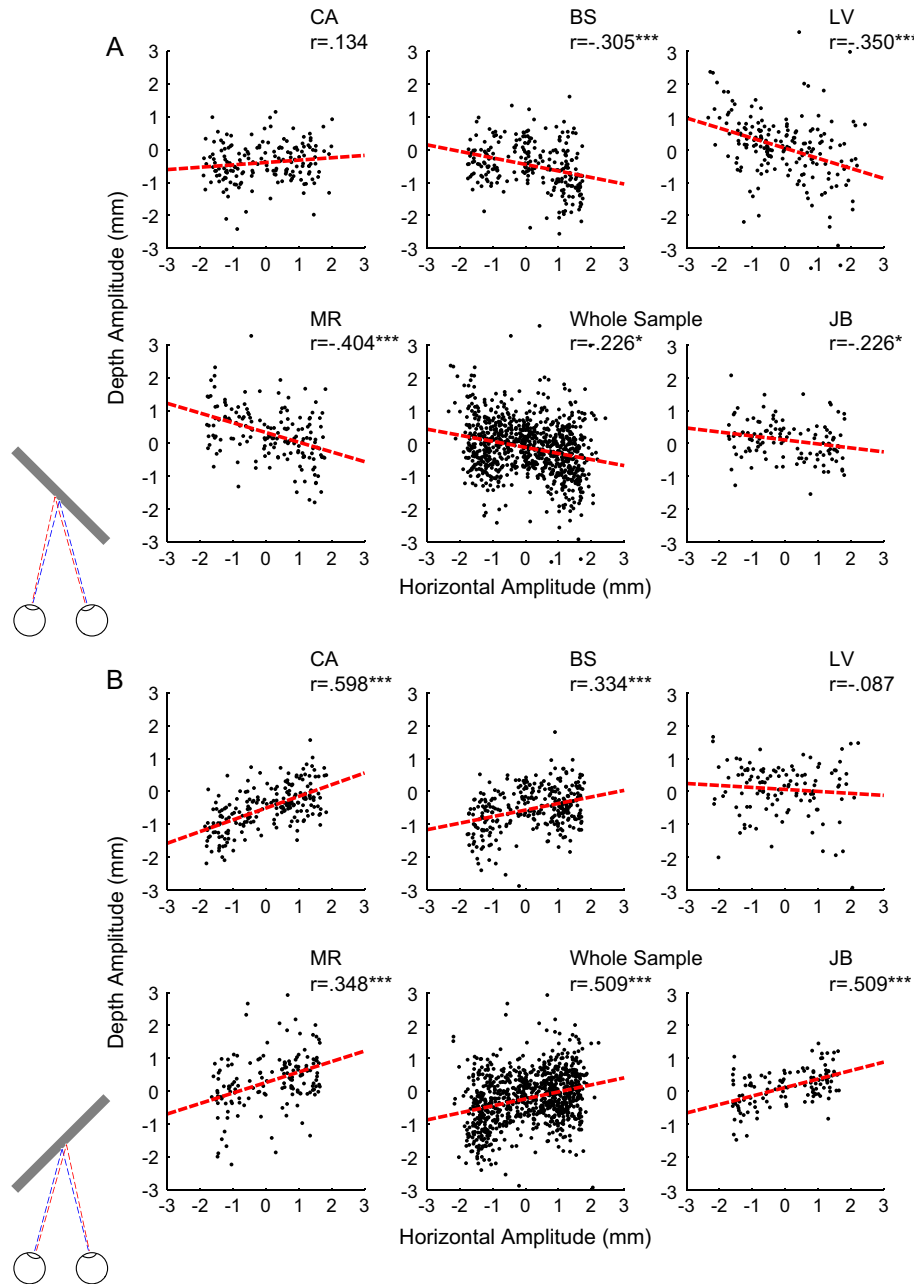
Fig. 16. Individual observer amplitudes of saccades on the horizontal plane. The saccades have been subsampled so as to have an average horizontal amplitude of under 0.97 mm (i.e. the average amplitude of the microsaccades we observed in the needle task). Saccades executed when the needle was oriented −45° and 45° are in panels A and B, respectively. Dashed lines are linear fits of the data. $^*p < .05$, $^{**}p < .01$, $^{***}p < .001$. All of the significant relationships as well as the relationship in the whole sample are in the expected direction.

(2) Microsaccade amplitude on the frontoparallel plane scales with the distance of the needle tip from its contact position.

(3) Microsaccades do not actuate a coordination of version and vergence in the natural task, whereas this is evident in the eye movements executed in the control task.

First of all, the observation of the average displacement of the point of gaze in the 2 s leading to contact suggests that the eyes preceded the needle tip. The fact that the eyes precede the hand or the hand-held object is a typical feature of oculomotor control in everyday tasks (Hayhoe et al., 2003; Land, 2006, 2009) and the fact that it is evident in a high-precision task suggests that the control of eye movements is actuated in a qualitatively similar way. In general, the pattern of eye movements we observed is entirely compatible with the one in the study by Ko, Poletti, and Rucci

(2010). Microsaccades occurred mostly when the distance between the task-relevant locations was comparable to the size of a microsaccade, and their amplitude scaled with this distance, which is a clear sign that the amplitude of microsaccades is controlled online, together with the position of the needle tip. Moreover, we found that the occurrence of microsaccades became less frequent immediately before contact, when the needle had almost reached the contact point, similar to the observations by Winterson and Collewijn (1976) and Bridgeman and Palca (1980). Again, these results are very much coherent with the idea that the pattern of eye movements in a task requiring high precision visuomotor control is qualitatively similar to the pattern observed in tasks requiring large-scale displacements of the hands and gaze (see Martinez-Conde, Otero-Millan, & Macknik, 2013) and in particular that microsaccades are used for visual exploration over small distances
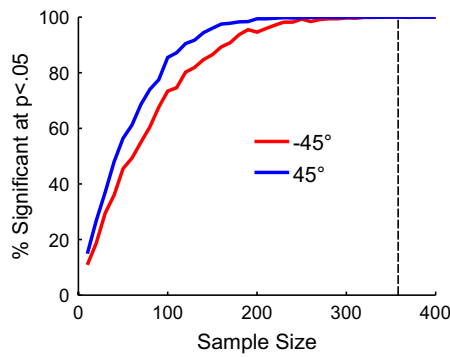
Fig. 17. Subsampling simulation. The red and blue curves represent the proportion of random sub-samples of the whole database where a significant correlation in the expected direction was found, as a function of sub-sample size, for the two orientations of the plane, respectively. The dashed vertical line represents the sample size of 358, i.e. the sample size in the needle experiment (see the whole sample plot in Fig. 12). Subsamples of 358 movements invariably yielded a significant relationship in the expected direction in the instructed saccade experiment. (For interpretation of the references to color in this figure legend, the reader is referred to the web version of this article.)

(Otero-Millan et al., 2013). In high-precision tasks microsaccades are used to displace gaze between the different task-relevant positions (Ko, Poletti, & Rucci, 2010), compensating for the changes in visual acuity within the fovea (Poletti, Listorti, & Rucci, 2013), much like saccades are used to target fixation on task-relevant objects in our daily activities (Hayhoe et al., 2003; Land, 2006, 2009). The hypothesis of a continuum between saccades and microsaccades is also supported by the increasing body of evidence showing that microsaccades, as well as large saccades, are triggered by activity in the Superior Colliculus (Goffart, Hafed, & Krauzlis, 2012; Hafed, 2011; Hafed & Krauzlis, 2012; Hafed, Goffart, & Krauzlis, 2009; Munoz & Wurtz, 1993).

The similarities between the small and large scale control of eye movements however did not prove to be complete as we started considering binocular coordination. It appears that in a task involving looking at or tapping objects at different depth levels (see Epelboim et al., 1995), despite a general tendency to hypovergence, the depth of the point of gaze is adjusted coherently with the distance of the fixated object, and most of the changes in vergence take place during saccades (Malinov et al., 2000). In our data on the contrary we did not observe any significant coordination of version and vergence during microsaccades. Although the needle tip in general approached the contact point on a slanted trajectory on the horizontal plane (i.e. moving towards a point farther and towards the left), the change in vergence associated with microsaccades was substantially unrelated to the change in version. This result contrasts with what we observed when we asked our observers to perform small saccades along a slanted plane. In this case we could show clear signs of coordination of version and vergence. The change in the vergence angle was consistent with the direction of saccades on the horizontal axis and with the orientation of the plane, also when the latter was congruent with the arrangement of the needle and target in the main experiment (i.e. rotated clockwise). Crucially, the relationship was evident both when we restricted the analysis to the saccades whose amplitude matched the one of the microsaccades we observed in the needle task, and to the saccades executed when the smallest movements (i.e. 1 mm) were instructed. This result implies first of all that our recording method, coupled with the 3D calibration approach, was in principle able to evidence very small adjustments of vergence had they been present. More importantly it suggests that the precise control of vergence is only actuated using fast eye movements if those are specifically instructed. Our data suggest that the control of vergence is actuated mostly by slow control in a high-precision

task. Notice that the results from the instructed saccade experiment do not exclude a role for slow control of vergence, on the contrary, both pre-saccadic and post-saccadic adjustments of vergence were evident together with the fast peri-saccadic adjustment.

As we mentioned in Section 1, the role of microsaccades in the control of binocular fixation has been a source of debate. Engbert and Kliegl (2004) reported a decrease in the amount of vergence error associated with microsaccades, whereas this was not evident in the study by Møller, Laursen, and Sjolie (2006). The evidence directly relating to tasks involving oculomotor control beyond the simple maintenance of fixation is also mixed. On one side Pérez Zapata, Aznar-Casanova, and Supèr (2013) found that the microsaccades occurring after a large scale saccade could correct the vergence error induced by a pictorial cue. On the other side Richter and Engbert (2013) found no change in vergence associated with microsaccades in a task requiring pursuit in depth. Our results confirm that small saccades can in principle actuate a fast control of vergence, coherently with the observation by Van Horn and Cullen (2012) that neurons in the oculomotor brainstem have the potential to trigger microsaccades in depth, but whether this is the case depends quite subtly on the task.

We suspect that the different binocular coordination between our instructed saccade task and our manual task might also depend on the visual properties of the display. For the instructed saccades we explicitly constructed a setup which would favor as much as possible the 3D targeting of saccades. Saccades were executed along a plane, with plenty of cues signaling the surface slant, not to mention the fact that the vertical marks we used as targets provided an optimal binocular disparity signal. In the manual task the cues to relative depth were quite impoverished, in particular neither the needle nor the target hole are associated with strong vertical edges. This could explain why microsaccades contributed to the correction of vergence error while looking at a strongly patterned stimulus in the data by Pérez Zapata, Aznar-Casanova, and Supèr (2013) but not relative to a point-like pursuit target in the results by Richter and Engbert (2013). Further research is needed to clarify exactly the conditions under which vergence control can be actuated through small fast eye movements. We think that the visual properties of the device we used in our task are quite representative of those we might face in a high-precision task in our daily experience. Under those conditions we predict that vergence will mostly be controlled through slow eye movements.

In summary, we were able to show that in a high precision task, version is controlled online to target gaze on the most task-relevant objects in the display, adapting to the movements of the hand. Vergence eye movements instead seem to be temporally decoupled from version movements and do not have the same function. Further studies should be aimed at establishing the precise conditions under which a coordinated control of binocular gaze takes place.

Acknowledgements

References

Bridgeman, B., & Palca, J. (1980). The role of microsaccades in high acuity observational tasks. *Vision Research, 20*(9), 813–817.

Challis, J. H. (1995). A procedure for determining rigid-body transformation parameters. *Journal of Biomechanics, 28*(6), 733–737.

Collewijn, H., & Kowler, E. (2008). The significance of microsaccades for vision and oculomotor control. *Journal of Vision, 8*(14).

Desmurget, M., Pelisson, D., Rossetti, Y., & Prablanc, C. (1998). From eye to hand: Planning goal-directed movements. *Neuroscience and Biobehavioral Reviews, 22*(6), 761–788.

Ditchburn, R. W. (1955). Eye-movements in relation to retinal action. *Optica Acta, 1*(4), 171–176.

Engbert, R., & Kliegl, R. (2003). Microsaccades uncover the orientation of covert attention. *Vision Research, 43*, 1035–1045.

Engbert, R., & Kliegl, R. (2004). Microsaccades keep the eyes' balance during fixation. *Psychological Science, 15*, 431–436.

Engbert, R., & Mergenthaler, K. (2006). Microsaccades are triggered by low retinal image slip. *Proceedings of the National academy of Sciences of the United States of America, 103*, 7192–7197.

Epelboim, J., Steinman, R. M., Kowler, E., Edwards, M., Pizlo, Z., Erkelens, C. J., et al. (1995). The function of visual-search and memory in sequential looking tasks. *Vision Research, 35*(23–24), 3401–3422.

Goffart, L., Hafed, Z. M., & Krauzlis, R. J. (2012). Visual fixation as equilibrium: Evidence from superior colliculus inactivation. *Journal of Neuroscience, 32*(31), 10627–10636.

Haddad, G. M., & Steinman, R. M. (1973). Smallest voluntary saccade – Implications for fixation. *Vision Research, 13*(6), 1075–1086.

Hafed, Z. M. (2011). Mechanisms for generating and compensating for the smallest possible saccades. *European Journal of Neuroscience, 33*(11), 2101–2113.

Hafed, Z. M., Goffart, L., & Krauzlis, R. J. (2009). A neural mechanism for microsaccade generation in the primate superior colliculus. *Science, 323*(5916), 940–943.

Hafed, Z. M., & Krauzlis, R. J. (2012). Similarity of superior colliculus involvement in microsaccade and saccade generation. *Journal of Neurophysiology, 107*(7), 1904–1916.

Hayhoe, M. M., Shrivastava, A., Mruczek, R., & Pelz, J. B. (2003). Visual memory and motor planning in a natural task. *Journal of Vision, 3*(1), 49–63.

Ko, H. K., Poletti, M., & Rucci, M. (2010). Microsaccades precisely relocate gaze in a high visual acuity task. *Nature Neuroscience, 13*(12), 1549–1553.

Kowler, E., & Steinman, R. M. (1977). Role of small saccades in counting. *Vision Research, 17*(1), 141–146.

Kowler, E., & Steinman, R. M. (1979). Miniature saccades – Eye-movements that do not count. *Vision Research, 19*(1), 105–108.

Land, M. F. (2006). Eye movements and the control of actions in everyday life. *Progress in Retinal and Eye Research, 25*(3), 296–324.

Land, M. F. (2009). Vision, eye movements, and natural behavior. *Visual Neuroscience, 26*(1), 51–62.

Malinov, I. V., Epelboim, J., Herst, A. N., & Steinman, R. M. (2000). Characteristics of saccades and vergence in two kinds of sequential looking tasks. *Vision Research, 40*(16), 2083–2090.

Martinez-Conde, S., Otero-Millan, J., & Macknik, S. L. (2013). The impact of microsaccades on vision: Towards a unified theory of saccadic function. *Nature Reviews Neuroscience, 14*(2), 83–96.

Mergenthaler, K., & Engbert, R. (2010). Microsaccades are different from saccades in scene perception. *Experimental Brain Research, 203*(4), 753–757.

Møller, F., Laursen, M. L., & Sjolie, A. K. (2006). The contribution of microsaccades and drifts in the maintenance of binocular steady fixation. *Graefes Archive for Clinical and Experimental Ophthalmology, 244*(4), 465–471.

Møller, F., Laursen, M. L., Tygesen, J., & Sjolie, A. K. (2002). Binocular quantification and characterization of microsaccades. *Graefes Archive for Clinical and Experimental Ophthalmology, 240*, 765–770.

Munoz, D. P., & Wurtz, R. H. (1993). Fixation cells in monkey superior colliculus. 1. Characteristics of cell discharge. *Journal of Neurophysiology, 70*(2), 559–575.

Otero-Milian, J., Troncoso, X. G., Macknik, S. L., Serrano-Pedraza, I., & Martinez-Conde, S. (2008). Saccades and microsaccades during visual fixation, exploration, and search: Foundations for a common saccadic generator. *Journal of Vision, 8*(14:21), 1–18.

Otero-Millan, J., Macknik, S. L., Langston, R. E., & Martinez-Conde, S. (2013). An oculomotor continuum from exploration to fixation. *Proceedings of the National academy of Sciences of the United States of America, 110*(15), 6175–6180.

Otero-Millan, J., Macknik, S., & Martinez-Conde, S. (2014). Fixational eye movements and binocular vision. *Frontiers in Integrative Neuroscience, 8*(00052).

Pérez Zapata, L., Aznar-Casanova, J. A., & Supèr, H. (2013). Two stages of programming eye gaze shifts in 3-D space. *Vision Research, 86*, 15–26.

Poletti, M., Listorti, C., & Rucci, M. (2013). Microscopic eye movements compensate for nonhomogeneous vision within the fovea. *Current Biology, 23*(17), 1691–1695.

Richter, E. M., & Engbert, R. (2013). Microsaccades do not correct for disparity error during smooth pursuit in depth. In *17th European conference on eye movements*, 6(3) (p. 564). Lund (Sweden): Journal of Eye Movement Research.

Sailer, U., Flanagan, J. R., & Johansson, R. S. (2005). Eye-hand coordination during learning of a novel visuomotor task. *Journal of Neuroscience, 25*(39), 8833–8842.

Schulz, E. (1984). Binocular micromovements in normal persons. *Graefes Archive for Clinical and Experimental Ophthalmology, 222*(2), 95–100.

Soderkvist, I., & Wedin, P. A. (1993). Determining the movements of the skeleton using well-configured markers. *Journal of Biomechanics, 26*(12), 1473–1477.

St.Cyr, G. J., & Fender, D. H. (1969). Interplay of drifts and flicks in binocular fixation. *Vision Research, 9*(2), 245–265.

Steinman, R. M., Haddad, G. M., Skavensky, A. A., & Wyman, D. (1973). Miniature eye-movement. *Science, 181*(4102), 810–819.

Theiler, J., Eubank, S., Longtin, A., Galdrikian, B., & Farmer, J. D. (1992). Testing for nonlinearity in time-series – The method of surrogate data. *Physica D: Nonlinear Phenomena, 58*(1–4), 77–94.

Timberlake, G. T., Wyman, D., Skavenski, A. A., & Steinman, R. M. (1972). The oculomotor error signal in the fovea. *Vision Research, 12*(5), 1059–1064.

Ukwade, M. T., Bedell, H. E., & Harwerth, R. S. (2003a). Stereopsis is perturbed by vergence error. *Vision Research, 43*(2), 181–193.

Ukwade, M. T., Bedell, H. E., & Harwerth, R. S. (2003b). Stereothresholds with simulated vergence variability and constant error. *Vision Research, 43*(2), 195–204.

Van Horn, M. R., & Cullen, K. E. (2012). Coding of microsaccades in three-dimensional space by premotor saccadic neurons. *Journal of Neuroscience, 32*(6), 1974–1980.

Wertheim, T. (1894). Über die indirekte Sehschärfe. *Zeitschrift für Psycholologie & Physiologie der Sinnesorgane, 7*, 172–187.

Winterson, B. J., & Collewijn, H. (1976). Microsaccades during finely guided visuomotor tasks. *Vision Research, 16*(12), 1387–1390.

Zuber, B. L., Stark, L., & Cook, M. (1965). Microsaccades and the velocity–amplitude relationship for saccadic eye movements. *Science, 150*, 1459–1460.